Published in final edited form as:
*J Org Chem*. 2009 July 3; 74(13): 4697–4704. doi:10.1021/jo900278g.

# Synthesis and Evaluation of Radamide Analogues, A Chimera of Radicicol and Geldanamycin

**M. Kyle Hadden** and **Brian S. J. Blagg***
Department of Medicinal Chemistry, The University of Kansas, 1251 Wescoe Hall Drive, Malott Hall 4070, Lawrence, Kansas 66045-7563

Brian S. J. Blagg: bblagg@ku.edu

## Abstract

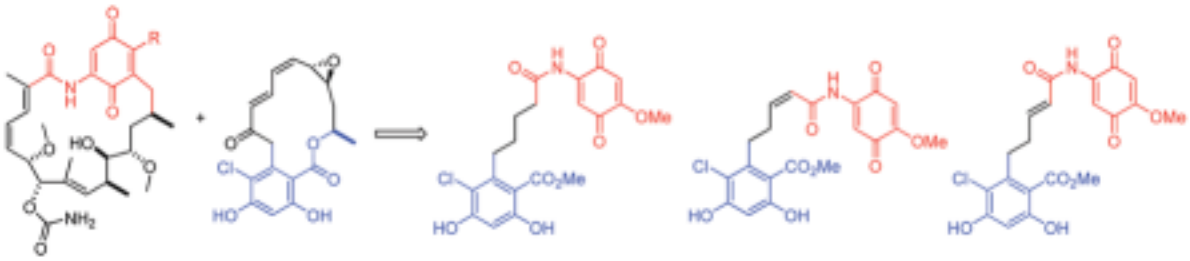

Previously, we reported the Hsp90 inhibitory activity of radamide, an open chain amide chimera of geldanamycin and radicicol. Attempts to further expand upon structure–activity relationships for this class of Hsp90 inhibitors led to the preparation of a series of radamide analogues focused on differing tether lengths and quinone mimics. In addition, the cup-shaped conformation adopted by the two natural products when bound to the Hsp90 N-terminal ATP binding pocket suggests that conformationally biased compounds may demonstrate improved binding and inhibition. The preparation and evaluation of radamide analogues with *cis*/*trans* α,*β*-unsaturated amides yielded compounds that exhibit improved antiproliferative activity. In addition, several analogues demonstrated the ability to induce degradation of Hsp90-dependent oncogenic signaling proteins in vitro, a hallmark of Hsp90 N-terminal inhibition.

## Introduction

Inhibition of the 90 kDa family of heat shock proteins (Hsp90) has become a major target for the development of anticancer drugs because of their well-defined role as molecular chaperones responsible for folding nascent polypeptides and refolding denatured proteins into their biologically active, three-dimensional conformations.[1] Numerous oncogenic proteins directly associated with all six hallmarks of cancer, including Her2, Raf, PLK, RIP, AKT, FAK, telomerase, and MET, have been shown to be dependent upon the Hsp90 protein folding machinery.2 Hsp90 inhibition results in the simultaneous disruption of multiple oncogenic pathways, leading to client protein degradation via the ubiquitin-proteasome pathway.

Known inhibitors of the Hsp90 protein folding process include the natural products, geldanamycin (GDA) and radicicol (RDC) (Figure 1). RDC, the most potent inhibitor in vitro,

*To whom correspondence should be addressed. Phone: 1-785-864-2288. Fax: 1-785-864-5326.

Supporting Information Available: Full characterization of key intermediates and all final analogues. This material is available free of charge via the Internet at http://pubs.acs.org.

exhibits no activity in vivo[3] as the allylic epoxide and the α, *β*, *γ*, *δ*-unsaturated ketone undergo nucleophilic addition that results in metabolites that exhibit little or no affinity for Hsp90. GDA, while less potent than RDC in vitro, maintains inhibitory activity in vivo.[4] In fact, an analogue of GDA, 17-AAG, exhibits enhanced affinity for tumorgenic Hsp90 and is currently in clinical trials for the treatment of various cancers. Unfortunately, 17-AAG exhibits poor solubility and toxicity that is proving difficult to overcome for this class of inhibitors.

Co-crystal structures of the Hsp90 N-terminal ATP binding site bound to RDC and GDA have provided information that was used to design chimeric inhibitors of Hsp90.[5] The resorcinolic phenols of RDC form hydrogen bonds with Leu34, Asp79, Gly83, and Thr171 through conserved water molecules, mimicking key interactions of the natural adenine base (Figure 1). In contrast, the quinone moiety of GDA binds toward the surface of the pocket in the region corresponding to the diphosphate group of ADP, providing hydrogen bonding interactions with Lys58 and Asp40. In addition, the 17-methoxy substituent of the GDA quinone and the RDC epoxide form hydrogen bonds with Lys44, emphasizing the importance of this amino acid in inhibitor binding. We hypothesized that incorporating the key binding interactions provided by the resorcinol ring of RDC and the quinone moiety of GDA into a single molecule would result in a novel class of Hsp90 inhibitors that could unveil structure–activity relationships (SAR) for the natural products themselves. Radamide (Figure 2) exhibited low micromolar inhibition of Hsp90 as measured by Her2 degradation in MCF-7 breast cancer cells.[6] Interestingly, the corresponding hydroquinone precursor demonstrated ~3-fold increased inhibition, suggesting that a hydrogen bond donor in the quinone binding region results in increased activity. Similar studies with the chimeric Hsp90 inhibitors, radester and radanamycin, further supported this finding, suggesting that the hydroquinone is more active in vitro.[7–9] This observation was later confirmed by researchers at Infinity Pharmaceuticals who identified the hydroquinone of GDA as the active form in vivo.[10] These initial findings suggest that modifications to the quinone moiety may provide analogues that demonstrate improved activity and decreased toxicity.

Santi and co-workers recently reported the co-crystal structure of 17-dimethylaminoethylamino geldanamycin (DMAG) bound to Hsp90 and performed a series of computational studies to understand the relationship between the bent conformation of GDA present in the ATP binding site versus its native conformation.[11] Their studies suggest that GDA binds Hsp90 and is twisted into a bent conformation by isomerization of the amide bond (*trans* → *cis*), which results in an entropic penalty between 2.2 and 6.4 kcal/mol. They further suggested that analogues of GDA that contain a *cis*-amide could exhibit >1000-fold increase in Hsp90 affinity. In contrast to GDA, RDC binds Hsp90 in a bent conformation identical to its native conformation and exhibits little entropic penalty.[5] Therefore, conformationally biased inhibitors that contain an α,*β*-unsaturated amide bond in either a *cis* or *trans* orientation represent inhibitors that are predisposed to a bent conformation and may exhibit improved inhibition. In this article, we describe the synthesis of saturated and unsaturated *cis*/*trans* α,*β*-unsaturated amides that incorporate quinone mimics along with their inhibitory activities.

## Results and Discussion

### Chemistry

The first series of radamide analogues prepared and evaluated were derivatives incorporating varying saturated alkyl linkers between the resorcinol and quinone moieties (Scheme 1). The hydroquinone and quinone analogues were prepared as previously described for radamide[6] and radanamycin[9] with minor modification (Scheme 1). Briefly, silyl protection and chlorination of 2,4-dihydroxy-5-methyl benzoate gave the fully protected resorcinolic ester **1**, which was used as an intermediate for subsequent analogues. Alkylation of **1** with appropriate alkenyl bromides and LDA furnished alkenes **2**–**4**. Conversion of the terminal olefins to the

corresponding carboxylic acids (**8**–**10**) and subsequent EDCI/DMAP-catalyzed coupling with the MOM-protected aniline[6] gave protected amides **12**–**14**. Deprotection of the resorcinol phenols, followed by removal of the MOM protecting groups via in situ generated trimethylsilyl iodide afforded a 1:1 mixture of the hydroquinone/quinone. The instability of the hydroquinone at room temperature resulted in significant oxidation to the quinone during chromatographic separation. Therefore, the mixture was subjected to air oxidation in the presence of palladium acetate immediately following MOM removal to furnish quinones **21**–**23**. Quantitative conversion of the quinone to the corresponding hydroquinones (**24**–**26**) was achieved by stirring with excess sodium hydrosulfite in EtOAc and $H_2O$ (50:50) for 20 min at room temperature. A library of radamide analogues (**44**–**56**) was prepared through EDCI/DMAP coupling of acids **5**–**7** with a variety of anilines (Schemes 2 and 3) chosen to probe SAR between the quinone and the ATP binding pocket.

Conformationally biased radamide analogue preparation commenced via a Still–Gennari modification of a Horner–Wadsworth–Emmons (HWE) reaction of aldehyde **5**. Utilizing bis (2,2,2-trifluoroethyl) (methoxycarbonylmethyl)phosphonate gave the *cis*-methyl ester **57** in good yield (Scheme 4). The corresponding *trans*-ester was formed through homologation procedures with triethyl phosphonoacetate and aldehyde **5** to give a 7:1 mixture of *trans*/*cis*-ethyl esters (Scheme 5). The *trans* isomer, **63**, was easily separated via flash chromatography, and both isomers were utilized in subsequent coupling steps. Trimethyl aluminum ($Me_3Al$)-mediated coupling of the ester and aniline **11**, followed by deprotection and oxidation/reduction steps described above, produced the *cis*- and *trans*-quinones, **61** and **68**, and hydroquinones, **62** and **69**. The anilines used for the saturated analogues were coupled to both ester isomers to furnish the respective *trans* (**79a**–**87a**) and *cis* (**79b**–**83b**) conformationally biased derivatives (Scheme 6).

The majority of anilines used to construct the conformationally biased amides were produced in good yields (>75%); however, the heterocyclic anilines were unreactive toward the *cis*-ester. In contrast, yields for the coupling of the same anilines with the *trans*-ester were moderate (30–48%, Table 1). These results suggested that orientation about the olefin was preventing attachment of the activated aniline due to steric congestion. Therefore, the corresponding *cis* analogues were prepared by alkylation of resorcinol **1** with propargyl bromide upon treatment with LDA to give the terminal alkyne, **88** (Scheme 7). **88** was inseparable from the starting material; however, after alkylation with methyl chloroformate, the resulting propargyl ester, **89**, cleanly separated from the starting ester under normal chromatographic conditions (34% overall for the two steps). Tri-methyl aluminum-mediated coupling of the alkyne ester with the heterocyclic anilines resulted in formation of the desired amides, **90a**–**c**, in good yields (63–85%), confirming steric congestion significantly retards this reaction.

The methyl ester aniline D (Table 1) required modification as described in the Experimental Section to prevent polymerization of this compound upon exposure to trimethyl aluminum. Reduced aniline activation times resulted in poor yields for *cis*-amide coupling. However, utilizing the alkyne ester, the desired compound **90d** was furnished in excellent yield (81%). The alkyne-linked compounds **90a**–**d** were treated with Lindlar's catalyst under a hydrogen atmosphere to give the corresponding *cis* isomer analogues in moderate yield. Finally, removal of the resorcinol protecting groups furnished the *cis*-radamide analogues **92a**–**d** in quantitative yield.

## Biological Results

Upon completion of the synthesis of radamide analogues **21**–**26**, **44**–**56**, **61**–**69**, **79a**–**87a**, **79b**–**83b**, and **92a**–**d**, their antiproliferative activities against two distinct human breast cancer cell lines, an estrogen receptor positive cell line, MCF-7, and an estrogen receptor negative, Her2 overexpressing cell line, SKBr3, were determined. In addition, each compound was tested

for its ability to decrease cellular levels of Her2, a Hsp90-dependent client protein involved with oncogenic signaling pathways in several types of cancer. The anilines utilized as quinone mimics (Scheme 3) were chosen to take advantage of the key interactions previously described for the Hsp90 N-terminal ATP binding site. In order to establish the optimal distance between the quinone and resorcinol moieties of radamide, a series of compounds containing an increasing number of methylene units were synthesized and evaluated (**21**–**26** and **44**–**49**). In addition, compounds **44**–**49** were also designed to determine whether the nitrile could provide additional hydrogen bonding interactions with Lys44 and improve Hsp90 inhibitory activity. The general trend for these compounds demonstrated that increasing tether length provided an increase in antiproliferative activity against both cell lines (Table 2). This was most evident when comparing the nitrile derivatives **44**–**49**, wherein each additional methylene resulted in the conversion of inactive analogues (**44** and **47**, $IC_{50} > 100$) into analogues with $IC_{50}$ values of ~30 $\mu$M against MCF-7 cells (Table 1). These results prompted the synthesis of a series of radamide analogues that contained a saturated four-carbon linker and the corresponding quinone mimics (**50**–**56**) that provided insight into the SAR for the quinone binding region. Analogues that contained no (**52**) or one (**50** and **54**) substituent exhibited poor antiproliferative activity, indicating the importance of having multiple interactions with the phosphate binding region. Substitution of the *para*-nitrile (**46**) with a *para*-methyl ester (**50**) resulted in two-fold decreased activity, suggesting that the nitrile at this position provides beneficial hydrogen bond acceptor properties. Comparison of the activities of compounds **46**, **49**, **51**, and **55** suggested that the pyridine/pyrazine nitrogens that were chosen to mimic the quinone oxygens are not essential for inhibitory activity when the nitrile is present. However, when absent, the pyridine nitrogens are important and may facilitate isomerization of the amide via their electron-withdrawing properties. These compounds were generally more active against MCF-7 cells, and overall, their ability to decrease Her2 levels in vitro correlated well with their antiproliferative activity against the SKBr3 cell line. Overall, the most active analogues contained the natural quinone/hydroquinone of GDA, prompting the design of a new class of radamide analogues that could demonstrate improved binding and inhibiton.

Because GDA and RDC bind Hsp90 in a bent conformation, it has been proposed that analogues of these natural products predisposed to this conformation will demonstrate improved Hsp90 binding affinity and subsequently exhibit higher inhibition in vitro.[11] Conformationally biased analogues of radamide containing an α,*β*-unsaturated amide bond in either a *cis* or *trans* orientation represent a class of inhibitors predisposed to a bent conformation that were prepared and tested for their Hsp90 inhibitory activity. Surprisingly, both the *cis*-quinone (**61**) and hydroquinone (**62**) were significantly less active in vitro than the corresponding *trans*-oriented analogues (quinone, **68**, and hydroquinone, **69**) (Table 3). In addition, both the *cis* and *trans* analogues demonstrated less antiproliferative activity compared to the corresponding saturated analogue, **26**. Taken together, these data suggest that increased rigidity of both the *cis* and *trans* orientations prevents the quinone from forming hydrogen bonding interactions with Asp40 and Lys98, which are observed upon GDA binding to Hsp90. The decrease in activity exhibited by these compounds also suggests that the orientation may provide improved interactions for various quinone mimics within the binding pocket. The antiproliferative activity exhibited by the conformationally biased analogues incorporating various quinone mimics provided additional insights into the SAR for this series of compounds (**79a**–**87a**, **79b**–**83b**, and **92a**–**d**, Table 3).

Similar to the saturated analogues, these compounds were generally more active against MCF-7 cells. In addition, the *trans*-oriented unsaturated compounds were slightly less active than the corresponding saturated quinone mimics, further supporting the SAR previously reported for both the quinone and the hydroquinone analogues. Direct comparison of the *cis*-and *trans*-oriented quinone mimics shows significant improvement in antiproliferative activity for the majority of *cis* compounds, suggesting that their predisposed bent conformation creates

improved binding interactions with Hsp90 or, at least, less entropic penalties upon binding. Five *cis* analogues demonstrated comparable (**83b**, **92b**, and **92d**) or improved (**79b** and **81b**) antiproliferative activity compared to the quinone/hydroquinone analogues in at least one in vitro assay. These quinone mimics also demonstrated the most potent inhibitory activity in the saturated series. Surprisingly, the *cis*-oriented analogue containing the *para*-nitrile, **79b**, was completely inactive against SKBr3 cells. This result, coupled with the increased activity observed for most compounds against the MCF-7 cell line, suggests that Hsp90 found in this cell line is more susceptible to drug treatment for some unknown reason. In a more direct determination of in vitro Hsp90 inhibition, Her2 degradation, the most active analogues were the *cis*- and *trans*-quinone/hydroquinones (**61**–**69**), which exhibited $IC_{50}$ values from ~35 to 57 $\mu$M.

On the basis of the data gathered for the radamide analogues, three compounds, **23**, **61**, and **81b**, were chosen for Western blot analyses based on their ability to induce degradation of Hsp90-dependent client proteins (Figure 3). Compounds **23** and **61** were chosen because they represent the most potent analogues from their respective series in both antiproliferative and Her2 degradation assays. Because these analogues contain the natural quinone, **81b** was also chosen for analysis as the most active *cis*-radamide analogue containing a quinone mimic (2,4,5-trifluoroaniline). Each compound induced degradation of Hsp90 client proteins in a concentration-dependent fashion and produced $IC_{50}$ values that correspond well with antiproliferative and Her2 results. Similar to results obtained for the antiproliferative and Her2 assays, the saturated four-carbon quinone **23** was most active and produced $IC_{50}$ values of ~25 $\mu$M. Both **61** and **81b** were less active, with $IC_{50}$ values of ~50–100 $\mu$M.

## Conclusion

Analogues of radamide, a chimeric Hsp90 inhibitor that contains the quinone ring of GDA and the resorcinol moiety of RDC linked through an amide bond, were prepared and evaluated. Increasing the length of the saturated chain analogues to four carbons resulted in increased activity for all analogues evaluated. Derivatives containing quinone mimics designed to investigate the importance of the various positions of the aromatic ring were generally less active than the natural quinone, highlighting its importance for optimal Hsp90 inhibitory activity. A series of *cis*-radamide analogues that are conformationally predisposed to adopt the cup shape necessary for high-affinity binding to the N-terminal ATP binding site were also designed, synthesized, and evaluated for Hsp90 inhibition. While these analogues demonstrated reduced Hsp90 inhibitory activity, several analogues were more active in antiproliferation assays, suggesting the potential for an alternative target for *cis* analogues. The design and synthesis of novel chimeric analogues that are conformationally biased toward the bent cup-shaped conformation is currently underway and will be reported in due course.

## Experimental Section

### 4-(3,5-Bis(*tert*-butyldimethylsilyloxy)-2-chloro-6-(methoxycarbonyl)phenyl)butanoic acid (9)

A solution of olefin **3** (454 mg, 0.909 mmol) was dissolved in 1,4-dioxane/$H_2O$ (40 mL, 3:1) at 25 °C. Osmium tetroxide (200 $\mu$L, 4% solution in $H_2O$) and sodium periodate (721 mg, 3.4 mmol) were added, and the mixture was stirred at 25 °C for 3 h. EtOAc (100 mL) and $H_2O$ (50 mL) were added to the mixture, and the aqueous layer was removed. The organic layer was washed with saturated aqueous NaCl (50 mL), dried ($Na_2SO_4$), filtered, and concentrated. Chromatography ($SiO_2$, 10:1, Hex/EtOAc) afforded **6** (375 mg, 82%) as a colorless oil. Aldehyde **6** (325 mg, 0.648 mmol) was dissolved in a solution of *tert*-butanol/2-methyl-2-butene/$H_2O$ (11.8 mL, 6:6:1). Sodium di-hydrogen phosphate (188 mg, 1.36 mmol) and sodium chlorite (94 mg, 1.04 mmol) were added to the solution at 25 °C. The mixture was stirred for 4 h and added directly to EtOAc (50 mL) and saturated aqueous $NaH_2PO_4$. The aqueous layer

was removed and the organic layer washed with $H_2O$ (50 mL) and saturated aqueous NaCl (50 mL), dried ($Na_2SO_4$), filtered, and concentrated. Chromatography ($SiO_2$, 3:1, Hex/EtOAc) afforded **9** as a clear oil in excellent yield (78%): $^1$H NMR ($CDCl_3$, 400 MHz) $\delta$ 6.31 (s, 1H), 3.85 (s, 3H), 2.74 (t, $J$ = 7.4 Hz, 2H), 2.43 (t, $J$ = 6.9 Hz, 2H), 1.94 (m, 2H), 1.05 (s, 9H), 0.95 (s, 9H), 0.33 (s, 6H), 0.31 (s, 6H); $^{13}$C NMR ($CDCl_3$, 125 MHz) $\delta$ 179.7 168.1, 152.9, 151.3, 138.5, 121.3, 118.6, 109.4, 52.2, 33.7, 31.1, 25.6 (3C), 25.5 (3C), 24.2, 18.3, 18.0, −4.3 (2C), −4.4 (2C); IR (film) $\nu_{max}$ 3022, 2806, 2776, 1732, 1713, 1586, 1468, 1410, 1362, 1254, 1199, 1108, 1042, 966, 939, 839 cm$^{-1}$; ESI-HRMS *m*/*z* calcd for $C_{24}H_{42}ClO_6Si_2$ $[M + H]^+$ 517.2208, found 517.2212.

### Methyl 4,6-Bis(*tert*-butyldimethylsilyloxy)-3-chloro-2-(4-(4-methoxy-2,5-bis (methoxymethoxy)phenylamino)-4-oxobutyl)-benzoate (13)

A solution of **11**[6] (648 mg, 2.7 mmol) in anhydrous $CH_2Cl_2$ (10 mL) was added to a mixture of 1-(3-dimethylaminopropyl)-3-ethylcarbodiimide hydrochloride (512 mg, 2.7 mmol), 4-dimethylaminopyridine (326 mg, 2.7 mmol), and **9** (457 mg, 0.89 mmol) in anhydrous $CH_2Cl_2$ (5 mL). The mixture was stirred for 12 h at 25 °C and concentrated under reduced pressure. Chromatography purification ($SiO_2$, 3:1, Hex/EtOAc) afforded **13** as a clear oil (448 mg, 68%): $^1$H NMR ($CDCl_3$, 400 MHz) $\delta$ 8.27 (s, 1H), 7.62 (s, 1H), 6.83 (s, 1H), 6.34 (s, 1H), 5.21 (s, 4H), 3.87 (s, 6H), 3.55 (s, 3H), 3.53 (S, 3H), 2.78 (t, $J$ = 8.0 Hz, 2H), 2.43 (t, $J$ = 7.4 Hz, 2H), 2.05 (m, 2H), 1.09 (s, 9H), 1.00 (s, 9H), 0.27 (s, 6H), 0.24 (s, 6H); $^{13}$C NMR ($CDCl_3$, 125 MHz) $\delta$ 170.2, 168.2, 152.9, 151.3, 146.2, 141.7, 140.8, 138.8, 121.7, 121.3, 118.7, 110.9, 109.4, 100.9, 96.3 (2C), 56.4 (2C), 56.3, 52.3, 37.3, 31.3, 25.6 (3C), 25.5 (3C), 25.1, 18.4, 18.0, −4.4 (2C), −4.5 (2C); IR (film) $\nu_{max}$ 3350, 2953, 2932, 2897, 2858, 2833, 1732, 1686, 1585, 1566, 1469, 1409, 1229, 1207, 995 cm$^{-1}$; ESI-HRMS *m*/*z* calcd for $C_{30}H_{45}ClN_3O_5Si_2$ $[M + H]^+$ 618.2586, found 618.2585.

### Methyl 3-Chloro-4,6-dihydroxy-2-(4-(4-methoxy-2,5-bis(methoxymethoxy)phenylamino)-4-oxobutyl)benzoate (16)

A solution of **13** (300 mg, 0.4 mmol) was dissolved in 10 mL of THF at rt. Tetrabutylammonium fluoride (2 mL of 1 M soln in THF, 2.0 mmol) was added and the mixture stirred for 1 h. Saturated $NH_4Cl$ (3 mL) was added and the aqueous layer washed three times with EtOAc (20 mL). The combined EtOAc layers were washed with saturated NaCl (5 mL), dried ($Na_2SO_4$), filtered, and concentrated. Chromatography ($SiO_2$, 1:1, Hex/EtOAc) afforded **16** as a white amorphous solid in excellent yield (170 mg, 82%): $^1$H NMR ($CDCl_3$, 400 MHz) $\delta$ 11.41 (s, 1H), 8.21 (s, 1H), 7.57 (s, 1H), 6.74 (s, 1H), 6.49 (s, 1H), 5.13 (s, 4H), 3.89 (s, 3H), 3.79 (s, 3H), 3.45 (s, 6H), 3.11 (t, $J$ = 8.2 Hz, 2H), 2.41 (t, $J$ = 7.3 Hz, 2H), 1.95 (m, 2H); $^{13}$C NMR ($CDCl_3$, 125 MHz) $\delta$ 171.1, 170.2, 163.1, 156.3, 146.3, 142.7, 141.6, 140.7, 121.4, 113.9, 110.6, 106.6, 102.6, 100.8, 96.4, 96.2, 56.5, 56.4, 56.3, 52.7, 37.8, 32.2, 32.3; IR (film) $\nu_{max}$ 3342, 2995, 2933, 1659, 1651, 1580, 1502, 1439, 1391, 1319, 1150, 1078, 991, 804 cm$^{-1}$; ESI-HRMS *m*/*z* calcd for $C_{23}H_{29}ClNO_{10}$ $[M + H]^+$ 514.1480, found 514.1490.

### Methyl 3-Chloro-4,6-dihydroxy-2-(4-(4-methoxy-3,6-dioxo-cyclohexa-1,4-dienylamino)-4-oxobutyl)benzoate (22)

A solution of **16** (35.7 mg, 0.07 mmol) and sodium iodide (105 mg, 0.7 mmol) was dissolved in anhydrous $CH_2Cl_2$/MeCN (5 mL, 1:1) under argon. Chlorotrimethylsilane (76 mg, 0.7 mmol) was added and the reaction stirred at rt for 30 min. The solvent was removed under reduced pressure and the crude mixture taken up in EtOAc (5 mL). Palladium acetate (10 mg) was added and the reaction stirred at Rt for 6 h. The solution was filtered through Celite, concentrated, and purified by preparative thin layer chromatography (1:2, Hex/EtOAC) to yield a yellow amorphous solid in modest yield (8.6 mg, 29% over two steps): $^1$H NMR (acetone-*d*, 400 MHz) $\delta$ 8.94 (s, 1H), 7.46 (s, 1H), 6.50 (s, 1H), 6.05 (s, 1H), 3.98 (s, 3H), 3.90 (s, 3H),

3.15 (t, *J* = 7.90 Hz, 2H), 2.77 (t, *J* = 7.2 Hz, 2H), 2.09 (m, 2H); $^{13}$C NMR (acetone-*d*, 125 MHz) $\delta$ 182.6, 181.9, 172.9, 170.7, 161.6, 159.9, 158.2, 142.7, 139.5, 128.5, 125.6, 111.6, 104.5, 102.2, 56.1, 51.9, 36.8, 31.4, 24.8; IR (film) $\nu_{max}$ 3306, 3194, 3090, 2952, 2927, 2853, 1709, 1657, 1599, 1499, 1414, 1319, 1173, 1128, 953, 877 cm$^{-1}$; ESI-HRMS *m*/*z* calcd for $C_{19}H_{19}ClNO_8$ $[M + H]^+$ 424.0799, found 424.0794.

### (*Z*)-Methyl 4,6-Bis(*tert*-butyldimethylsilyloxy)-3-chloro-2-(5-methoxy-5-oxopent-3-enyl) benzoate (57)

18-Crown-6 (3.99 g, 15 mmol) and bis(2,2,2-trifluoroethyl) (methoxycarbonylmethyl) phosphonate (677 $\mu$L, 3.2 mmol) were cooled to −78 °C in anhydrous THF. KHMDS (10 mL of a 0.5 M solution in toluene, 5 mmol) was added dropwise and the solution stirred at −78 °C for 1 h. A solution of **5** (1.18 g, 2.5 mmol) in anhydrous THF (10 mL) was added dropwise and the solution stirred at −78 °C for 3 h. The solution was warmed to rt, diluted with EtOAc (50 mL), and saturated $NH_4Cl$ (50 mL) and the aqueous layer removed. The organic layer was washed with $H_2O$ (50 mL), saturated NaCl (50 mL), dried ($Na_2SO_4$), filtered, and concentrated. Chromatography ($SiO_2$, 20:1, Hex/EtOAc) afforded **57** as a clear oil in good yield (842 mg, 62%): $^1$H NMR ($CDCl_3$, 400 MHz) $\delta$ 6.32 (s, 1H), 6.24 (m, 1H), 5.78 (d, *J* = 11.4 Hz, 1H), 3.87 (s, 3H), 3.70 (s, 3H), 2.94 (m, 2H), 2.80 (t, *J* = 7.6 Hz, 2H), 1.05 (s, 9), 0.95 (s, 9H), 0.22 (s, 6H), 0.20 (s, 6H); $^{13}$C NMR ($CDCl_3$, 125 MHz) $\delta$ 168.1, 166.6, 152.9, 151.3, 148.5, 138.2, 121.3, 119.9, 118.7, 109.5, 52.1, 51.0, 30.9, 28.7, 25.6 (3C), 25.5 (3C), 18.4, 18.0, −4.3 (2C), −4.4 (2C); IR (film) $\nu_{max}$ 2962, 2932, 2897, 2843, 2858, 1724, 1643, 1585, 1557, 1470, 1356, 1266, 1163, 1097, 1042, 960, 783 cm$^{-1}$; ESI-HRMS *m*/*z* calcd for $C_{26}H_{44}ClO_6Si_2$ $[M + H]^+$ 544.2257, found 544.2264.

### (*Z*)-Methyl 4,6-Bis(*tert*-butyldimethylsilyloxy)-3-chloro-2-(5-(4-methoxy-2,5-bis (methoxymethoxy)phenylamino)-5-oxopent-3-enyl)benzoate (58)

To a solution of **11** (101 mg, 0.42 mmol) in anhydrous $CH_2Cl_2$ (5 mL) at 0 °C was added trimethylaluminum (0.42 mmol, 2 M in toluene). The mixture was warmed to 25 °C for 1 h before dropwise addition to a solution of **57** (93.7 mg, 0.17 mmol) and potassium carbonate (310 mg, 2.2 mmol) in anhydrous $CH_2Cl_2$ at 0 °C. The mixture was warmed to 25 °C and stirred for 3 h before quenching via the dropwise addition of saturated $NaHCO_3$ (5 mL) solution. $H_2O$ (10 mL) and EtOAc (15 mL) were added, and the aqueous layer was removed. The organic layer was washed with saturated NaCl (5 mL), dried ($Na_2SO_4$), filtered, and concentrated. Chromatography (SiO2, 5:1, Hex/EtOAc) afforded **58** as a yellow oil in good yield (62%): $^1$H NMR ($CDCl_3$, 400 MHz) $\delta$ 8.31 (s, 1H), 7.63 (s, 1H), 6.31 (s, 1H), 6.12 (m, 1H), 5.87 (d, *J* = 11.4 Hz, 1H), 5.20 (s, 2H), 5.18 (s, 2H), 3.88 (s, 3H), 3.86 (s, 3H), 3.54 (s, 3H), 3.50 (s, 3H), 3.04 (m, 2H), 2.85 (d, *J* = 7.9 Hz, 2H), 1.05 (s, 9H), 0.95 (s, 9H), 0.23 (s, 6H), 0.21 (s, 6H); $^{13}$C NMR ($CDCl_3$, 125 MHz) $\delta$ 168.2, 163.7, 152.9, 151.3, 146.3, 144.9, 141.5, 140.8, 138.4, 123.3, 121.8, 121.4, 118.7, 110.5, 109.4, 100.8, 96.2 (3C), 56.4, (2C), 52.2, 31.2, 28.4, 25.6 (3C), 25.5 (3C), 18.4, 18.0, −4.3 (2C), −4.4 (2C); IR (film) $\nu_{max}$ 2953, 2932, 2897, 2858, 1732, 1680, 1585, 1468, 1408, 1355, 1207, 1151, 995, 941, 679 cm$^{-1}$; ESI-HRMS *m*/*z* calcd for $C_{36}H_{57}ClNO_{10}Si_2$ $[M + H]^+$ 754.3209, found 754.3212.

### (*E*)-Methyl 4,6-Bis(*tert*-butyldimethylsilyloxy)-3-chloro-2-(5-ethoxy-5-oxopent-3-enyl) benzoate (63)

Triethyl phosphonoacetate (1.34 g, 6.0 mmol) in anhydrous THF was cooled to −78 °C. LiHMDS (6 mL of a 1.0 M solution, 6.0 mmol) was added dropwise and the solution warmed to rt for 5 min. The solution was recooled to −78 °C, and **5** (1.1 g, 2.4 mmol) in anhydrous THF was added dropwise and the solution stirred for 2 h. The solution was warmed to rt, diluted with EtOAc (50 mL), and saturated $NH_4Cl$ (50 mL) and the aqueous layer removed. The organic layer was washed with $H_2O$ (50 mL), saturated NaCl (50 mL), dried ($Na_2SO_4$), filtered,

and concentrated. Chromatography ($SiO_2$, 20:1, Hex/EtOAc) afforded 600 mg of a 7:1 mixture of *trans: cis* (**63**/**64**) isomers as a clear oil (60% overall yield). Further chromatography of this mixture ($SiO_2$, $CH_2Cl_2$) afforded pure *trans* and *cis* iosmers: $^1$H NMR ($CDCl_3$, 400 MHz) $\delta$ 6.95–7.05 (m, 1H), 6.32 (s, 1H), 5.85 (d, $J$ = 15.7 Hz, 1H), 4.20 (q, 2H), 3.86 (s, 3H), 2.79 (t, $J$ = 7.6 Hz, 2H), 2.48 (m, 2H), 1.30 (t, $J$ = 7.5 Hz, 3H), 1.05 (s, 9H), 0.95 (s, 9H), 0.26 (s, 6H), 0.23 (s, 6H); $^{13}$C NMR ($CDCl_3$, 100 MHz) $\delta$ 168.0, 166.6, 153.0, 151.4, 147.8, 138.1, 121.7, 121.1, 118.5, 109.6, 60.2, 52.2, 31.9, 30.7, 25.6 (3C), 25.5 (3C), 18.4, 18.0, 14.3, −4.3 (2C), −4.4 (2C); IR (film) $\nu_{max}$ 2955, 2896, 2888, 1726, 1656, 1566, 1431, 1410, 1253, 1198, 1105, 1042, 841, 783 cm$^{-1}$; ESI-HRMS *m*/*z* calcd for $C_{27}H_{46}ClO_6Si_2$ $[M + H]^+$ 557.2521, found 557.2535.

### (*Z*)-Methyl 4,6-Bis(*tert*-butyldimethylsilyloxy)-3-chloro-2-(5-ethoxy-5-oxopent-3-enyl) benzoate (64)

$^1$H NMR ($CDCl_3$, 400 MHz) $\delta$ 6.33 (s, 1H), 6.23 (m, 1H), 5.77 (d, $J$ = 11.4 Hz, 1H), 4.16 (q, $J$ = 7.3 Hz, 3H), 3.85 (s, 3H), 2.96 (m, 2H), 2.81 (t, $J$ = 7.3 Hz, 2H), 1.29 (t, $J$ = 7.2 Hz, 2H), 1.05 (s, 9H), 0.95 (s, 9H), 0.23 (s, 6H), 0.21 (s, 6H); $^{13}$C NMR ($CDCl_3$, 100 MHz) $\delta$ 168.1, 166.2, 152.9, 151.3, 148.3, 138.4, 121.3, 120.3, 118.7, 109.5, 59.8, 52.1, 30.9, 28.6, 25.6 (3C), 25.5 (3C), 18.4, 18.0, 14.3, −4.3 (2C), −4.4 (2C); IR (film) $\nu_{max}$ 2953, 2932, 2897, 2887, 2858, 1724, 1643, 1585, 1557, 1470, 1356, 1254, 1163, 1097, 1042, 960, 783 cm$^{-1}$; ESI-HRMS *m*/*z* calcd for $C_{27}H_{46}ClO_6Si_2$ $[M + H]^+$ 557.2521, found 557.2244.

### Methyl 2-(But-3-ynyl)-4,6-bis(*tert*-butyldimethylsilyloxy)-3-chlorobenzoate (88)

**1** (5.88 g, 13.1 mmol) was dissolved in anhydrous THF and cooled to −78 °C. Lithium diisopropyl amide (8.56 mL of a 2 M solution, 17.1 mmol) was added and the mixture stirred at −78 °C for 5 min. Propargyl bromide (12.5 g, 105 mmol) was added dropwise, and the solution was warmed to rt over 2 h. The solution was diluted with EtOAc (75 mL) and saturated $NH_4Cl$ (75 mL) and the aqueous layer removed. The organic layer was washed with $H_2O$ (75 mL), saturated NaCl (75 mL), dried ($Na_2SO_4$), filtered, and concentrated. Chromatography ($SiO_2$, 50:1, Hex/EtOAc) afforded a 1:3 mixture of **1** and **88** as a clear oil that was inseparable on a scale larger than 20 mg: $^1$H NMR ($CDCl_3$, 400 MHz) $\delta$ 6.30 (s, 1H), 3.85 (s, 3H), 2.90 (t, $J$ = 8.2 Hz, 2H), 2.44 (t, $J$ = 7.9 Hz, 2H), 1.97 (s, 1H), 1.05 (s, 9H), 0.95 (s, 9H), 0.23 (s, 6H), 0.21 (s, 6H); $^{13}$C NMR ($CDCl_3$, 125 MHz) $\delta$ 167.9, 153.0, 151.5, 137.5, 121.2, 118.7, 109.8, 83.5, 68.5, 52.3, 31.5, 25.6 (3C), 25.5 (3C), 18.5, 18.4, 18.0, −4.3 (2C), −4.4 (2C); IR (film) $\nu_{max}$ 3311, 2929, 2858, 2120, 1732, 1585, 1470, 1361, 1253, 1202, 1108, 962, 842 cm$^{-1}$; ESI-HRMS *m*/*z* calcd for $C_{24}H_{40}ClO_4Si_2$ $[M + H]^+$ 483.2153, found 483.2135.

### Methyl 4,6-Bis(*tert*-butyldimethylsilyloxy)-3-chloro-2-(5-methoxy-5-oxopent-3-ynyl) benzoate (89)

A mixture of **1** and **88** (1.635 g, 3.4 mmol) was dissolved in anhydrous THF and cooled to −78 °C. Lithium diisopropyl amide (2.2 mL of a 2 M solution, 4.4 mmol) was added and the mixture stirred at −78 °C for 5 min. Methyl chloroformate (2.1 mL, 33.9 mmol) was added dropwise, and the solution was warmed to rt over 2 h. The solution was diluted with EtOAc (75 mL) and saturated $NH_4Cl$ (75 mL) and the aqueous layer removed. The organic layer was washed with $H_2O$ (75 mL), saturated NaCl (75 mL), dried ($Na_2SO_4$), filtered, and concentrated. Chromatography ($SiO_2$, 50:1, Hex/EtOAc) afforded **89** as a pure yellow solid (34% overall two steps from **1**): mp = 78 °C; $^1$H NMR ($CDCl_3$, 400 MHz) $\delta$ 6.29 (s, 1H), 3.84 (s, 3H), 3.73 (s, 3H), 2.92 (d, $J$ = 7.9 Hz, 2H), 2.59 (d, $J$ = 8.1 Hz, 2H), 1.01 (s, 9H), 0.92 (s, 9H), 0.21 (s, 6H), 0.19 (s, 6H); $^{13}$C NMR ($CDCl_3$, 125 MHz) $\delta$ 167.8, 154.2, 153.1, 151.6, 136.7, 121.2, 118.6, 109.9, 88.5, 73.0, 52.6, 52.4, 30.4, 25.6 (3C), 25.4 (3C), 18.6, 18.3, 18.0, −4.3 (2C), −4.4 (2C); IR (film) $\nu_{max}$ 2953, 2932, 2887, 2241, 1715, 1585, 1567, 1470, 1433, 1252, 1093, 961 cm$^{-1}$; ESI-HRMS *m*/*z* calcd for $C_{26}H_{42}ClO_6Si_2$ $[M + H]^+$ 541.2208, found 541.2203.

### Methyl 4,6-Bis(*tert*-butyldimethylsilyloxy)-3-chloro-2-(5-(4-(methoxycarbonyl) phenylamino)-5-oxopent-3-ynyl)benzoate (90d)

To a solution of methyl 4-aminobenzoate (176 mg, 1.16 mmol) in anhydrous $CH_2Cl_2$ (5 mL) at 0 °C was added trimethylaluminum (1.16 mmol, 2 M in toluene), and the mixture was stirred for 3 min before dropwise addition to a solution of **89** (125.5 mg, 0.23 mmol) and potassium carbonate (416 mg, 3.0 mmol) in anhydrous $CH_2Cl_2$ at 0 °C. The mixture was warmed to 25 °C and stirred for 3 h before quenching via the dropwise addition of saturated $NaHCO_3$ (5 mL) solution. $H_2O$ (10 mL) and EtOAc (15 mL) were added, and the aqueous layer was removed. The organic layer was washed with saturated NaCl (5 mL), dried ($Na_2SO_4$), filtered, and concentrated. Chromatography (SiO2, 3:1, Hex/EtOAc) afforded **90d** as a yellow oil in excellent yield (81%): $^1$H NMR ($CDCl_3$, 400 MHz) $\delta$ 9.34 (s, 1H), 7.98 (d, $J$ = 8.6 Hz, 2H), 7.69 (d, $J$ = 8.6 Hz, 2H), 6.38 (1H), 3.94 (s, 3H), 3.89 (s, 3H), 2.96 (t, $J$ = 6.1 Hz, 2H), 2.78 (t, $J$ = 6.5 Hz, 2H), 1.05 (s, 9H), 0.95 (s, 9H), 0.23 (s, 6H), 0.21 (s, 6H); $^{13}$C NMR ($CDCl_3$, 100 MHz) $\delta$ 169.1, 166.7, 153.4, 151.6, 151.2, 142.4, 136.4, 130.7 (2C), 125.4, 121, 118.8, (2C), 118.6, 109.8, 86.7, 76.8, 52.8, 52.2, 29.9, 25.6 (3C), 25.4 (3C), 18.3, 18.0, 17.9, −4.3 (2C), −4.4 (2C); IR (film) $\nu_{max}$ 2952, 2932, 2858, 2231, 1721, 1280, 1661, 1587, 1531, 1433, 1256, 1111, 1044, 841, 901, 678 cm$^{-1}$; ESI-HRMS $m/z$ calcd for $C_{33}H_{47}ClNO_7Si_2$ $[M + H]^+$ 660.2580, found 660.2591.

### (*Z*)-Methyl 4,6-Bis(*tert*-butyldimethylsilyloxy)-3-chloro-2-(5-(5-cyanopyridin-2-ylamino)-5-oxopent-3-enyl)benzoate (91a)

A solution of **90a** (47.5 mg, 0.08 mmol) and Lindlar's catalyst (10 wt %) EtOAc (2 mL) was stirred at room temperature for 1 h under a $H_2$ atmosphere. The mixture was filtered through a plug of Celite. Chromatography ($SiO_2$, 10:1, Hex/EtOAc) afforded **91a** in moderate yield as a clear oil (48%): $^1$H NMR ($CDCl_3$, 400 MHz) $\delta$ 8.56 (s, 1H), 8.43 (d, $J$ = 8.7 Hz, 1H), 8.16 (s, 1H), 7.94 (dd, $J$ = 8.8, 2.2 Hz, 1H), 6.33 (m, 2H), 5.89 (d, $J$ = 11.5 Hz, 1H), 3.88 (s, 3H), 3.08 (m, 2H), 2.87 (t, $J$ = 8.1 Hz, 2H), 1.05 (s, 9H), 0.95 (s, 9H), 0.23 (s, 6H), 0.21 (s, 6H); $^{13}$C NMR ($CDCl_3$, 100 MHz) $\delta$ 168.2, 164.2, 154.0, 153.0, 151.6, 151.5, 149.2, 141.4, 138.1, 121.7, 121.2, 118.7, 116.9, 113.4, 109.5, 104.7, 52.2, 30.9, 28.7, 25.6 (3C), 25.5 (3C), 18.4, 18.0, −4.3 (2C), −4.4 (2C); IR (film) $\nu_{max}$ 3546, 2867, 2116, 1666, 1543, 1495, 1267, 1225, 1028, 956 cm$^{-1}$; ESI-HRMS $m/z$ calcd for $C_{31}H_{45}ClN_3O_5Si_2$ $[M + H]^+$ 630.2586, found 630.2571.

### Antiproliferation and Her2 Degradation Assays

These assays for Hsp90 inhibition were performed as described previously.[12]

### Western Blot Analyses of Naphthoquinones

MCF-7 cells were seeded ($1 \times 10^6$/plate) in culture dishes and allowed to attach overnight. Compounds **23**, **61**, and **81b** were added at varying concentration and incubated (37 °C, 5% $CO_2$) for 24 h. Cells were harvested and analyzed for Hsp90 client protein degradation as described previously.[9]

## Supplementary Material

Refer to Web version on PubMed Central for supplementary material.

## Acknowledgments

This work was supported by the National Institutes of Health (CA109265) and the Kansas Cancer Center (Postdoctoral Fellowship, M.K.H.).

## References


1. Blagg BS, Kerr TD. Med Res Rev 2006;26:310–338. [PubMed: 16385472]
2. Maloney A, Workman P. Expert Opin Biol Ther 2002;2:3–24. [PubMed: 11772336]
3. Geng X, Yang ZQ, Danishefsky SJ. Synlett 2004;8:1325–1333.
4. Supko JG, Hickman RL, Grever MR, Malspeis L. Cancer Chemother Pharmacol 1995;36:305–315. [PubMed: 7628050]
5. Roe SM, Prodromou C, O'Brien R, Ladbury JE, Piper PW, Pearl LH. J Med Chem 1999;42:260–266. [PubMed: 9925731]
6. Clevenger RC, Blagg BSJ. Org Lett 2004;6:4459–4462. [PubMed: 15548050]
7. Shen G, Blagg BSJ. Org Lett 2005;7:2157–2160. [PubMed: 15901158]
8. Wang M, Shen G, Blagg BSJ. Bioorg Med Chem Lett 2006;16:2459–2462. [PubMed: 16464590]
9. Shen G, Wang M, Welch TR, Blagg BSJ. J Org Chem 2006;71:7618–7631. [PubMed: 16995666]
10. Adams, J.; Gao, Y.; Evangelinos, ATG.; Grenier, L.; Pak, RH.; Porter, JR.; Wright, JL. US Patent Appl Publ. 2006. US 2006019941, A1 20060126, CAN 144: 170823 AN 2006: 74768
11. Jez JM, Chen JCH, Rastelli G, Stroud RM, Santi DV. Chem Biol 2003;10:361–368. [PubMed: 12725864]
12. Hadden MK, Hill SA, Davenport J, Matts RL, Blagg BSJ. Bioorg Med Chem 2009;17:634–640. [PubMed: 19101151]

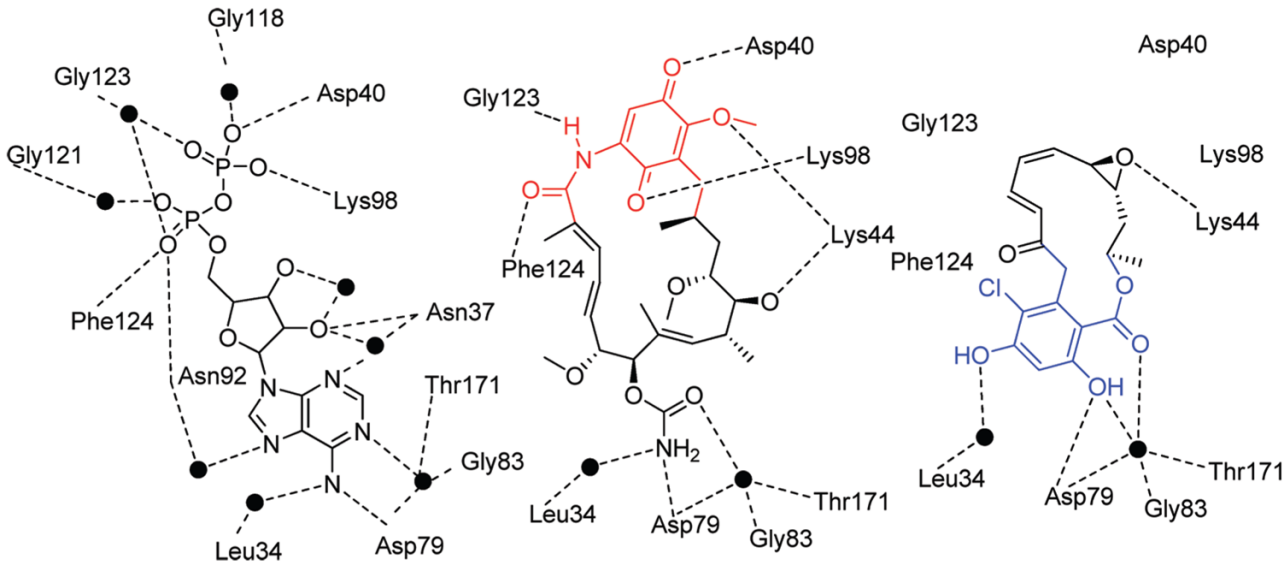


**Figure 1.**
Key interactions of ADP, GDA, and RDC with the Hsp90 N-terminal ATP binding pocket.

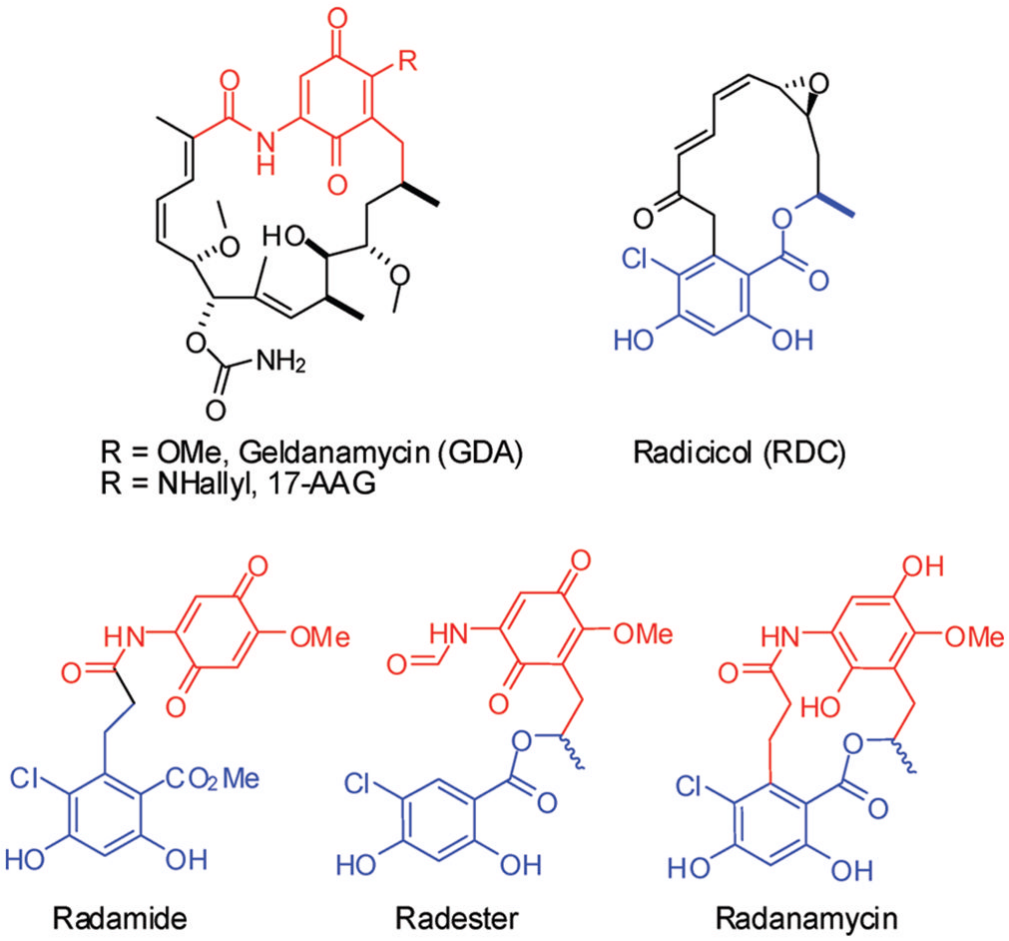


**Figure 2.**
Structures of chimeric Hsp90 inhibitors.

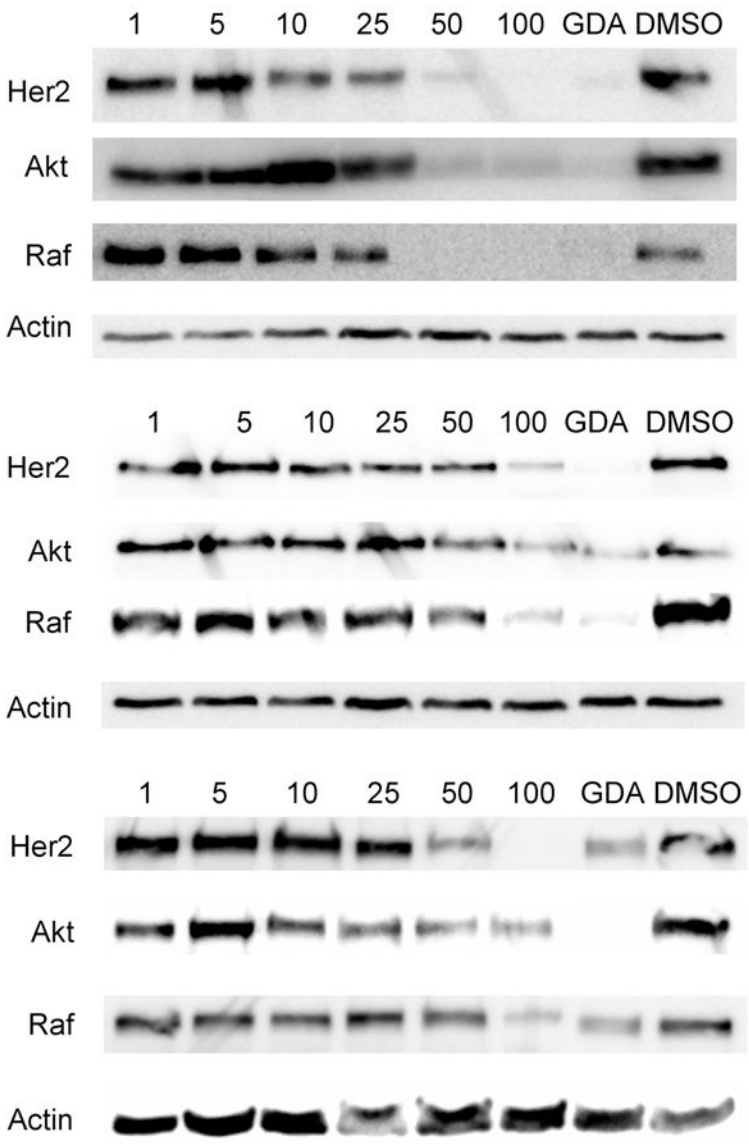


**Figure 3.**
Hsp90 client protein degradation induced by **23** (top), **61** (middle), or **81b** (bottom). Compound, at varying concentrations ($\mu$M), was evaluated for its ability to downregulate several client proteins as described in the Experimental Section. GA (500 nM) and DMSO were used as positive and negative controls, respectively.

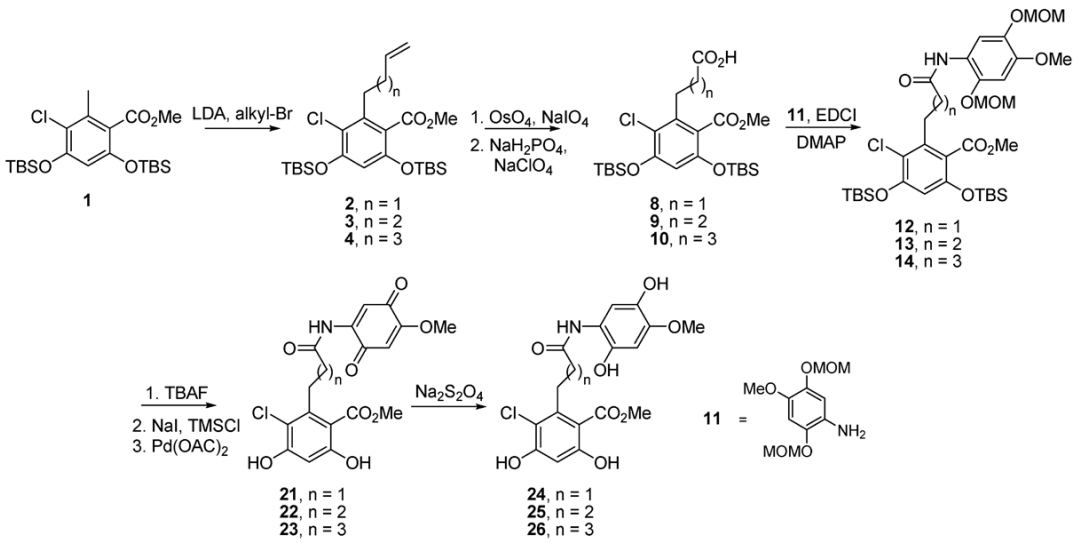


**Scheme 1.**

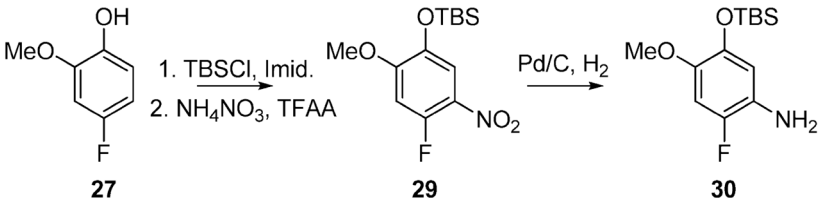


**27** **29** **30**

**Scheme 2.**

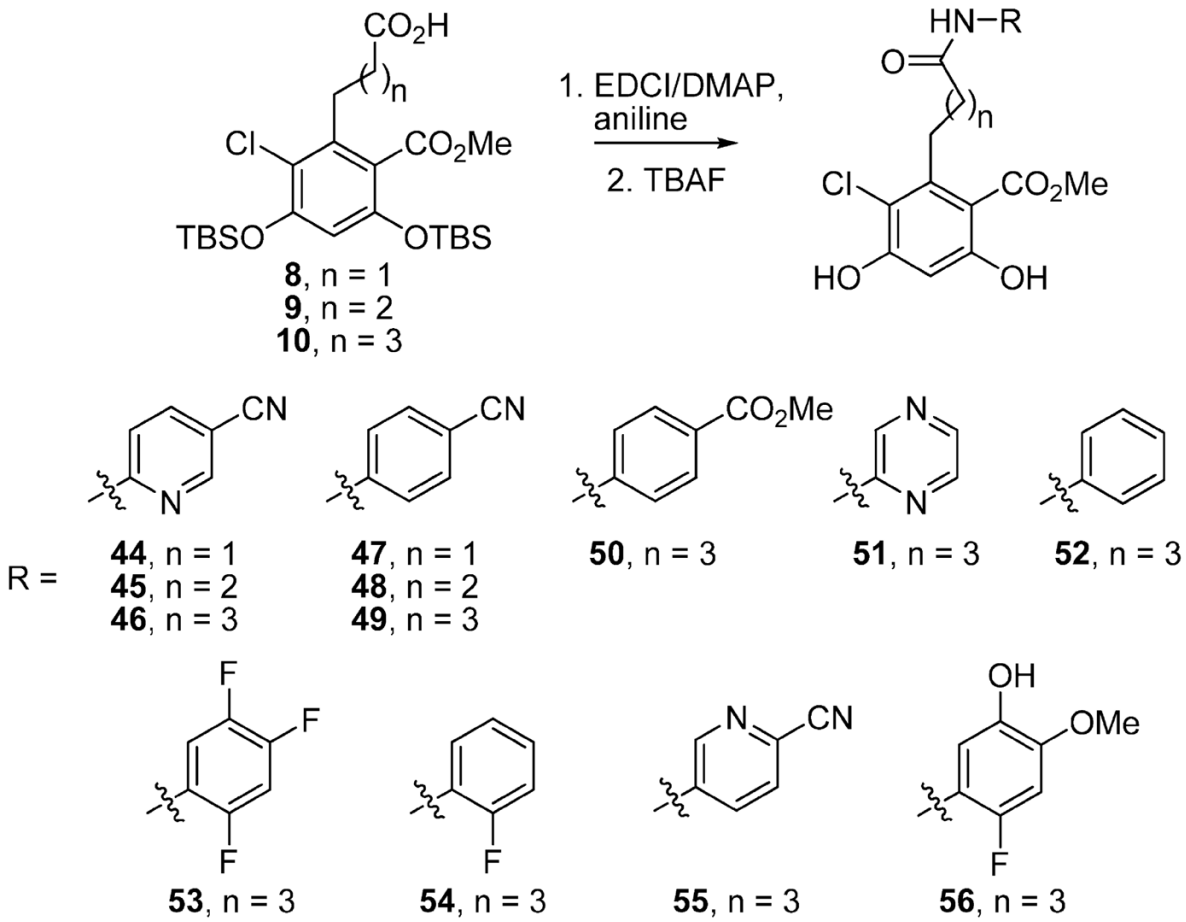


**Scheme 3.**

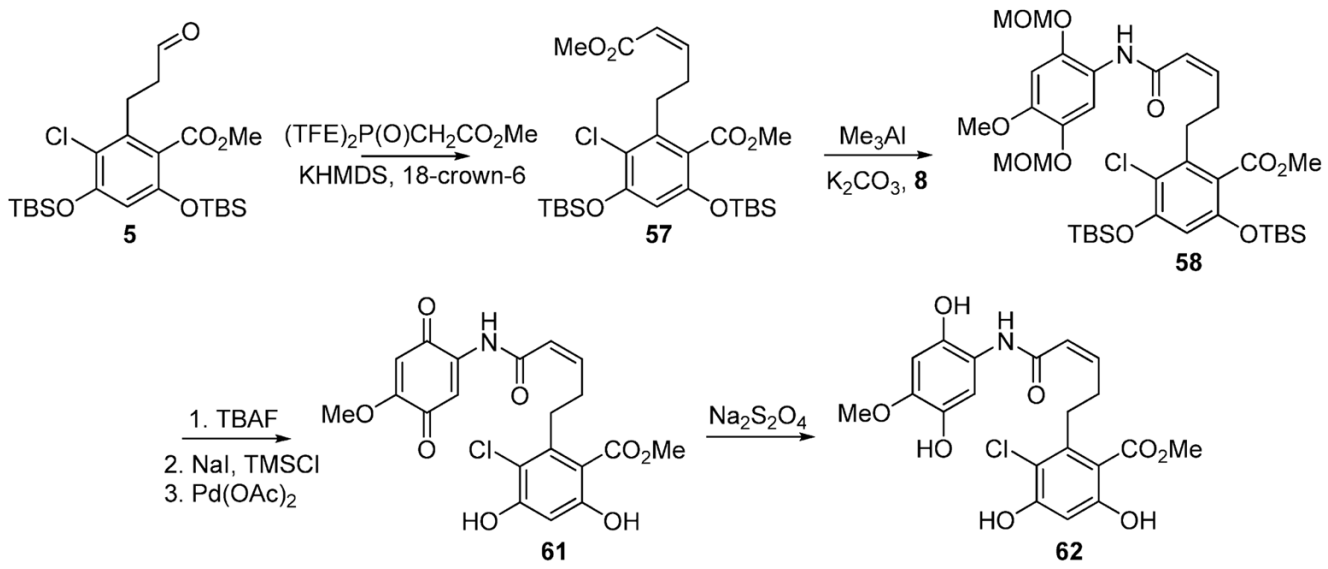


**Scheme 4.**

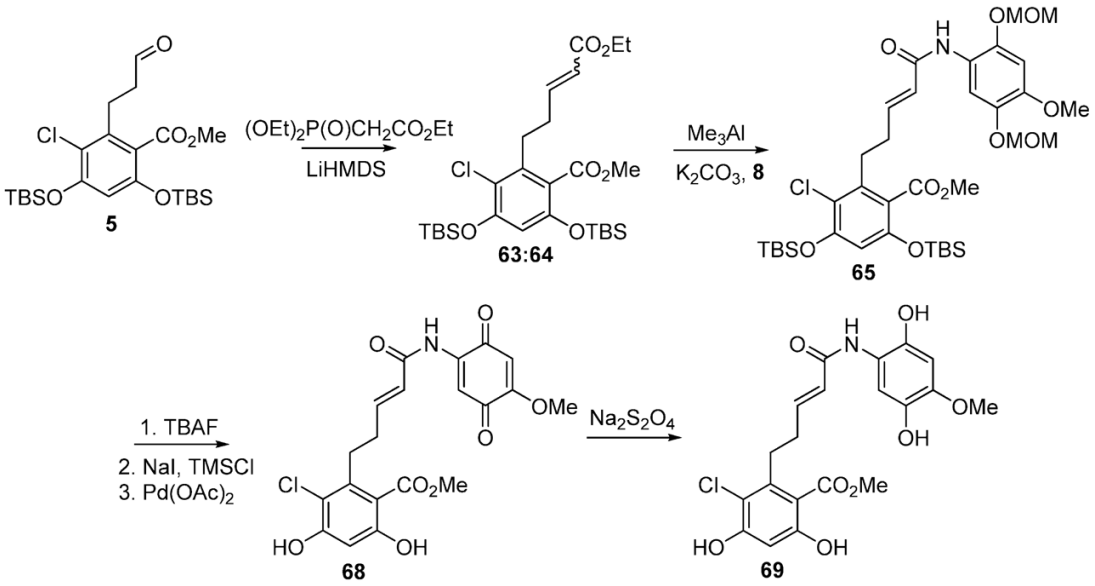


**Scheme 5.**

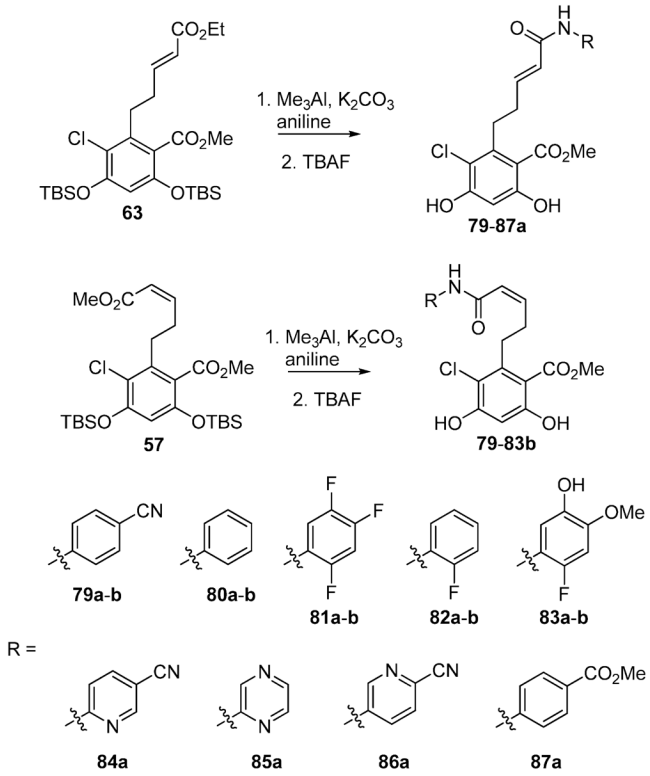


**Scheme 6.**

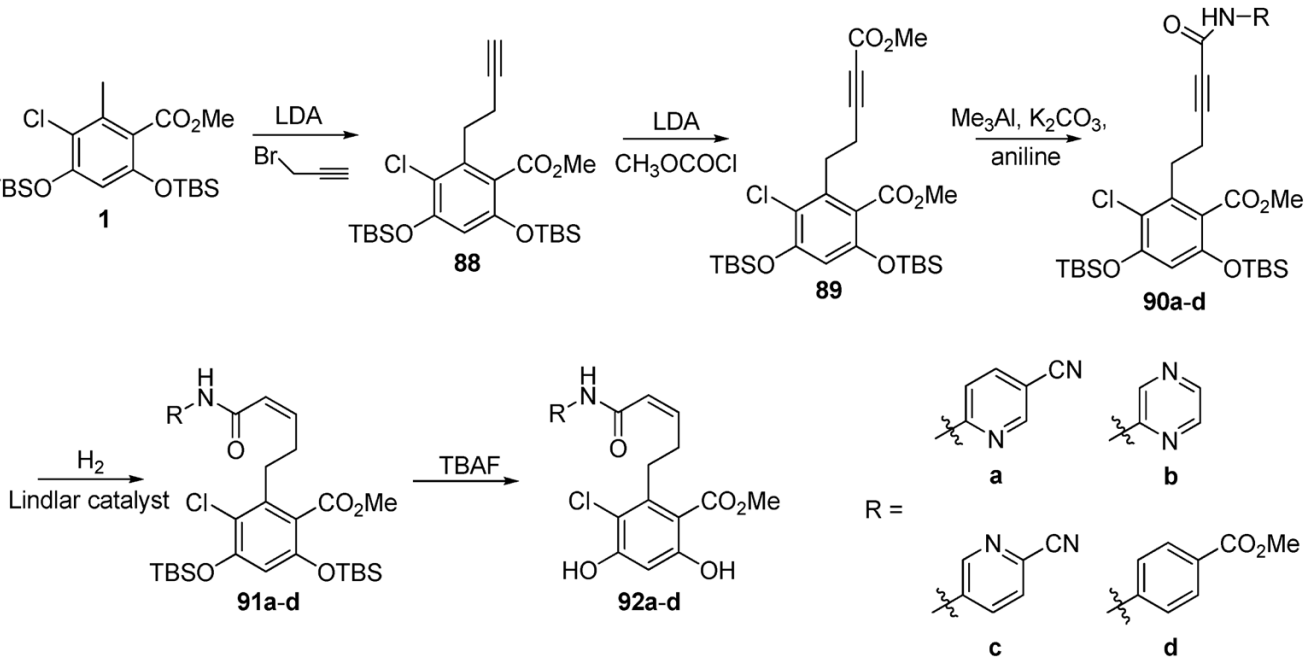


**Scheme 7.**

**Table 1**

Yield of Trimethyl Aluminum Couplings for Heterocyclic Anilines

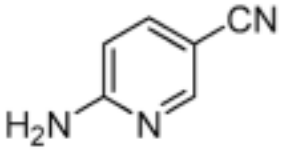


A

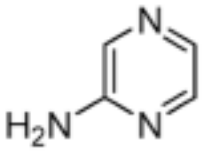


B

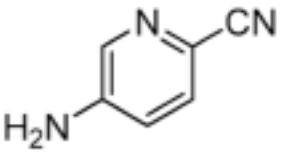


C

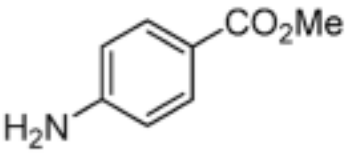


D

| aniline | *cis*-ester | *trans*-ester | alkyne ester |
|---|---|---|---|
| A | 0% | 30% | 85% |
| B | 0% | 28% | 75% |
| C | 0% | 48% | 63% |
| D | 2% | 31% | 81% |

**Table 2**

In Vitro Activities of Radamide Analogues with Varying Length Saturated Chain[a]

| compound | MCF-7 | SKBr3 | Her2 ELISA |
|---|---|---|---|
| **21** | 18.6 ± 0.9 | 23.7 ± 1.7 | 16.3 ± 5.0 |
| **22** | 12.9 ± 0.2 | 13.4 ± 1.2 | 12.1 ± 3.3 |
| **23** | 11.9 ± 0.6 | 13.0 ± 0.7 | 13.0 ± 3.1 |
| **24** | 14 ± 1.4 | 23.0 ± 1.2 | 16.2 ± 5.7 |
| **25** | 11.9 ± 0.4 | 14.5 ± 0.8 | 12.8 ± 1.7 |
| **26** | 11.6 ± 0.8 | 12.4 ± 0.4 | 20.5 ± 2.7 |
| **44** | >100 | >100 | >100 |
| **45** | 74.9 ± 0.8 | >100 | 83.2 ± 6.8 |
| **46** | 30.6 ± 3.5 | 51.6 ± 0.3 | 47.8 ± 1.7 |
| **47** | >100 | >100 | >100 |
| **48** | 87.4 ± 1.7 | >100 | 60.5 ± 7.1 |
| **49** | 33.0 ± 0.2 | 47.1 ± 0.4 | 48.3 ± 2.4 |
| **50** | 78.1 ± 4.4 | 91.6 ± 1.8 | 61.8 ± 9.0 |
| **51** | 43.0 ± 1.6 | 42.7 ± 4.8 | 46.4 ± 0.7 |
| **52** | 84.6 ± 4.5 | 97.8 ± 1.5 | >100 |
| **53** | 54.9 ± 1.0 | 54.0 ± 0.8 | 37.3 ± 7.8 |
| **54** | 71.8 ± 9.1 | 75.1 ± 5.5 | 63.5 ± 4.9 |
| **55** | 72.5 ± 6.9 | >100 | 92.3 ± 2.4 |
| **56** | 30.5 ± 1.2 | 45.9 ± 0.5 | 29.9 ± 2.7 |

[a]All values are the mean ± SEM of at least two separate experiments performed in triplicate.

**Table 3**

In Vitro Activities of Conformationally Biased Radamide Analogues[a]

| compound | MCF-7 | SKBr3 | Her2 ELISA |
|---|---|---|---|
| **61** | 25.5 ± 7.6 | 38.7 ± 3.6 | 34.9 ± 0.4 |
| **62** | 45.5 ± 4.0 | 71.1 ± 4.1 | 35.1 ± 2.7 |
| **68** | 18.5 ± 0.3 | 44.1 ± 5.7 | 56.5 ± 4.2 |
| **69** | 16.5 ± 2.7 | 26.7 ± 1.8 | 37.5 ± 1.3 |
| **79a** | 66.7 ± 4.0 | 70.7 ± 8.2 | 90.6 ± 2.1 |
| **79b** | 7.0 ± 1.6 | >100 | >100 |
| **80a** | 79.3 ± 15 | 95.7 ± 1.3 | 80.0 ± 2.4 |
| **80b** | >100 | >100 | >100 |
| **81a** | 61.7 ± 3.2 | 80.5 ± 9.5 | 88.1 ± 9.5 |
| **81b** | 14.2 ± 2.0 | 54.9 ± 2.8 | 65.8 ± 3.3 |
| **82a** | 82.4 ± 3.9 | >100 | >100 |
| **82b** | >100 | >100 | >100 |
| **83a** | >100 | >100 | >100 |
| **83b** | 20.2 ± 0.6 | 46.9 ± 6.6 | 69.5 ± 2.1 |
| **84a** | 52.5 ± 2.7 | 53.2 ± 4.2 | 62.3 ± 6.1 |
| **85a** | 72.6 ± 6.1 | 45.9 ± 6.4 | 58.3 ± 4.5 |
| **86a** | 87.6 ± 5.0 | >100 | >100 |
| **87a** | 35.1 ± 6.0 | 32.6 ± 6.5 | 64.9 ± 3.4 |
| **92a** | 46.1 ± 6.3 | 58.9 ± 6.6 | 68.5 ± 8.8 |
| **92b** | 26.4 ± 3.2 | >100 | >100 |
| **92c** | 40.6 ± 2.0 | 82.9 ± 3.3 | >100 |
| **92d** | 20.9 ± 2.4 | 78.1 ± 1.7 | 94.4 ± 2.2 |

[a] All values are the mean ± SEM of at least two separate experiments performed in triplicate.